

# COGNOS: Universal Enhancement for Time Series Anomaly Detection via Constrained Gaussian-Noise Optimization and Smoothing

Wenlong Shang<sup>1</sup>, Peng Chang<sup>1,2,\*</sup>,

<sup>1</sup>School of Information Science and Technology, Beijing University of Technology

<sup>2</sup>Beijing Key Laboratory of Computational Intelligence and Intelligent System, Beijing University of Technology  
shangwl@emails.bjut.edu.cn, changpeng@emails.bjut.edu.cn

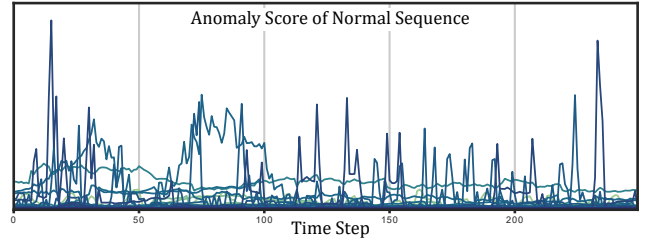
## Abstract

Reconstruction-based methods are a dominant paradigm in time series anomaly detection (TSAD), however, their near-universal reliance on Mean Squared Error (MSE) loss results in statistically flawed reconstruction residuals. This fundamental weakness leads to noisy, unstable anomaly scores with a poor signal-to-noise ratio, hindering reliable detection. To address this, we propose Constrained Gaussian-Noise Optimization and Smoothing (COGNOS), a universal, model-agnostic enhancement framework that tackles this issue at its source. COGNOS introduces a novel Gaussian-White Noise Regularization strategy during training, which directly constrains the model’s output residuals to conform to a Gaussian white noise distribution. This engineered statistical property creates the ideal precondition for our second contribution: a Kalman Smoothing Post-processor that provably operates as a statistically optimal estimator to denoise the raw anomaly scores. The synergy between these two components allows COGNOS to robustly separate the true anomaly signal from random fluctuations. Extensive experiments demonstrate that COGNOS is highly effective, delivering an average F-score uplift of 57.9% when applied to 12 diverse backbone models across multiple real-world benchmark datasets. Our work reveals that directly regularizing output statistics is a powerful and generalizable strategy for significantly improving anomaly detection systems.

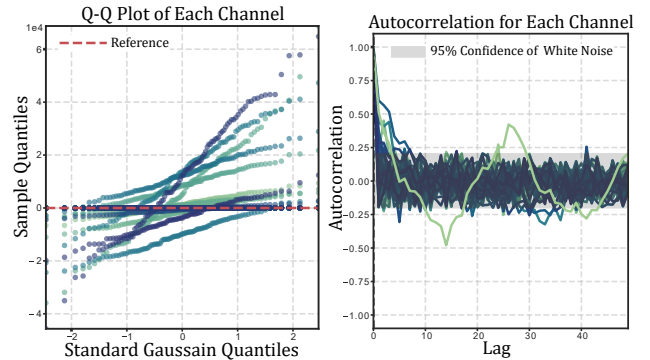
## Introduction

Time series anomaly detection (TSAD) is a critical task across numerous real-world domains, including monitoring for industrial manufacturing, ensuring financial system security, and maintaining the stability of IT infrastructure (Zamanzadeh Darban et al. 2024), where the timely identification of deviations from normal behavior is essential for preventing catastrophic failures and significant losses. In recent years, self-supervised reconstruction-based methods have become the dominant paradigm. A wide range of deep learning architectures, from classic autoencoders to sophisticated transformer-based models, have been employed within this framework (Wang et al. 2024b). These models are trained on vast amounts of normal data to learn a compressed representation of typical patterns, with the goal of accurately reconstructing normal sequences while failing to reconstruct anomalous ones.

\*Corresponding Author



(a) Noisy Anomaly Score



(b) Non-Gaussian Residuals

(c) Correlated Residuals

Figure 1: Limitations of standard MSE-based training for anomaly detection, illustrated using a Transformer on the SWaT dataset. (a) The resulting anomaly score is highly noisy, creating a poor signal-to-noise ratio where true anomalous deviations are masked. (b) The Q-Q plot reveals that reconstruction residuals are strongly non-Gaussian, indicating poorly modeled underlying noise. (c) The autocorrelation plot shows significant temporal correlation remaining in the residuals, suggesting the model failed to capture all predictable patterns.

Despite their architectural diversity and success, the training objective that forms the cornerstone of these methods is mostly the Mean Squared Error (MSE) loss. This reliance on MSE leads to two fundamental limitations. First, the raw anomaly scores derived from MSE often exhibit a poor signal-to-noise ratio, making it difficult to distinguish true anomalies from random fluctuations. Second, and more

fundamentally, the reconstruction residuals, which are the very source from which the anomaly score is derived, often possess undesirable statistical properties. As illustrated in Fig. 1, these issues reveal that standard models fail to fully separate deterministic patterns from random noise, ultimately hindering detection performance.

Recognizing the limitations of MSE, recent research has explored alternative objectives, largely centered around contrastive learning, to enhance representation quality. These methods encourage the model to pull representations of similar samples together while pushing dissimilar ones apart. While effective at learning more discriminative representations, these approaches are often coupled with specific model architectures or data manipulation methods and do not directly address the statistical nature of the final reconstruction residuals, which are the ultimate source of the anomaly score.

To address these challenges at their core, we propose **COGNOS**, a universal enhancement framework for time series anomaly detection that operates through **CO**nstrained **G**aussian-**N**oise **O**ptimization and **S**oothing. Our approach introduces a novel Gaussian-White Noise Regularization strategy during model training. Instead of focusing on the latent representation space, our regularizer directly constrains the reconstruction residuals to conform to a Gaussian white noise distribution. This novel objective fundamentally improves model generalization and produces residuals with ideal statistical properties. Building upon this, our second key contribution is a Kalman Smoothing Post-processor designed to denoise the anomaly scores. The central innovation lies in the synergistic effect between these two components: our regularization strategy creates the ideal statistical conditions (Gaussian, uncorrelated noise) under which the Kalman smoother can provably operate as a statistically optimal estimator. This allows it to robustly separate the true anomaly signal from random fluctuations. As a result, our model-agnostic framework can be universally applied to enhance existing reconstruction models.

Our contributions are as follows:

- We propose a novel Gaussian-White Noise Regularization strategy that directly enforces desirable statistical properties on reconstruction residuals, a fundamentally different approach from existing representation-focused contrastive methods.
- We design a Kalman Smoothing post-processor that acts in synergy with our regularization, leveraging the engineered residual properties to achieve optimal denoising of anomaly scores and significantly improve stability.
- We demonstrate that COGNOS is model-agnostic, and through extensive experiments on multiple state-of-the-art architectures and real-world benchmark datasets, we confirm its effectiveness, showing consistent and significant gains in anomaly detection performance.

## Related Work

### Time Series Anomaly Detection Models

Self-supervised time series anomaly detection (TSAD) is dominated by reconstruction-based methods. These have

evolved from classic Autoencoders (AE) (Kieu et al. 2022) and LSTMs (Liu et al. 2022a) to advanced Transformer-based architectures (Xu et al. 2022) and models that fuse time-frequency representations (Wu et al. 2023; Wang et al. 2024a). Further advancements include techniques like integrating frequency patching (Wu et al. 2025) and leveraging graph neural networks (Huang et al. 2025). A parallel research direction is contrastive learning, which aims to improve representation quality by contrasting samples in the latent space using techniques like temporal neighborhood sampling (Tonekaboni, Eytan, and Goldenberg 2021; Franceschi, Dieuleveut, and Jaggi 2019; Darban et al. 2025), cross-view prediction (Eldele et al. 2021; Yang et al. 2023b), or hierarchical contrasting (Yue et al. 2022). These works primarily innovate on **model architectures** or **latent space learning objectives**. In contrast, COGNOS is a model-agnostic enhancement that addresses a more fundamental issue: the suboptimal statistical properties of the final reconstruction residuals.

### Filtering and Regularization Techniques for Time Series Anomaly Detection

Another stream of research seeks to improve robustness through filtering or regularization. One approach integrates filters directly into the model, such as using deep filters to preprocess inputs (Yu et al. 2024), or coupling models with a Kalman Filter to create new hybrid architectures (Ma et al. 2024; Huang et al. 2023). Another approach applies regularization during training, often targeting the latent representation space by constraining feature learning with SVD (Yao et al. 2024) or enforcing periodic consistency (Yang et al. 2023a). COGNOS differs fundamentally from both paradigms. Instead of creating new integrated models or regularizing latent representations, it introduces a novel regularization directly on the final **output residuals**. This strategy engineers the ideal statistical properties needed for a provably optimal **post-processing** smoother, a distinct approach from prior work.

## Methodology

We propose a novel two-stage, model-agnostic framework (Fig. 2) to enhance reconstruction-based time series anomaly detection. The first stage applies **Gaussian-White Noise Regularization (GWRN)** during training, compelling reconstruction residuals of normal data to follow Gaussian white noise properties for improved generalization and normalcy representation. The second stage uses a **Kalman Smoothing Post-processor** to denoise raw anomaly scores into stable, discriminative signals. Critically, GWRN creates ideal Gaussian, uncorrelated residuals, enabling the smoother to optimally separate true anomalies from noise. Below, we detail the composite regularization objective and post-processing pipeline.

### Gaussian-White Noise Regularization

Reconstruction-based anomaly detection relies on learning the normal data manifold, where residuals for normal samples should ideally resemble random noise without structure

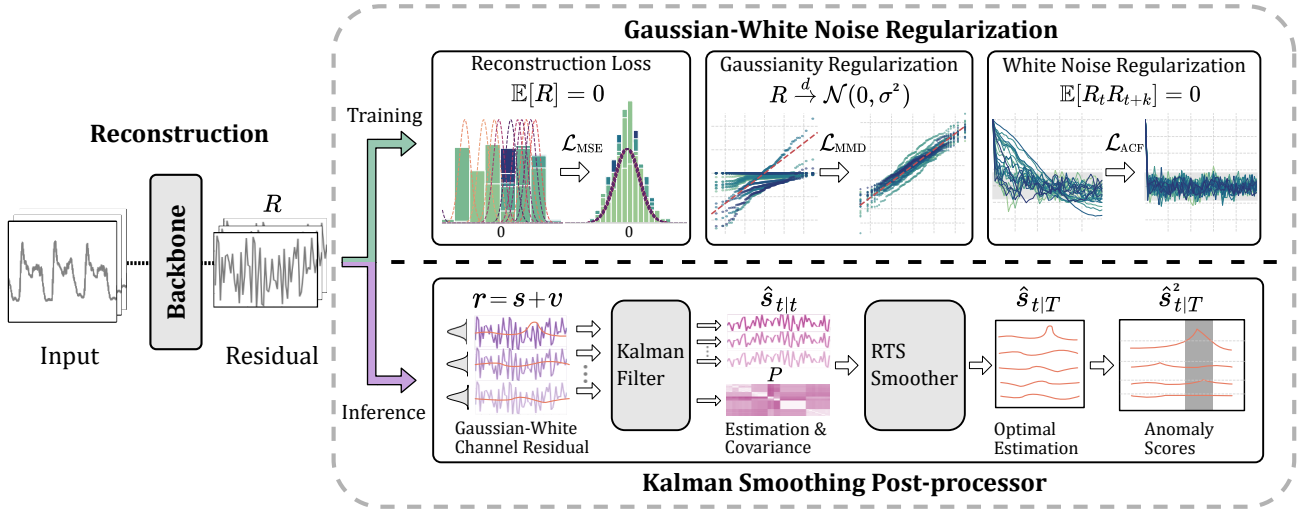


Figure 2: COGNOS Overview: Backbones are trained with Gaussian white noise regularization, and residuals are then post-processed using a Kalman smoother to generate stable anomaly scores.

or temporal patterns. We formalize this via GWN, which explicitly shapes residuals to Gaussian white noise properties, which is a key prerequisite for optimal Kalman smoothing in the next section. The total loss combines three objectives: a foundational reconstruction loss, a distributional regularizer for Gaussianity, and a temporal regularizer for white noise.

**Reconstruction Loss ( $\mathcal{L}_{\text{MSE}}$ ).** We employ the standard Mean Squared Error (MSE) to ensure the model’s output  $\hat{x}$  maintains high fidelity to the input  $x$ . This serves as the primary driver for learning the data’s deterministic patterns, calculated over all individual elements of the reconstruction residual  $R = x - \hat{x}$  as follows:

$$\mathcal{L}_{\text{MSE}} = \frac{1}{|R|} \sum_{r \in R} r^2. \quad (1)$$

**Gaussianity Regularization ( $\mathcal{L}_{\text{MMD}}$ ).** To enforce that residuals of normal data lack complex underlying structures, we regularize their empirical distribution to match a target Gaussian distribution,  $\mathcal{N}(0, \sigma^{*2})$ . We use the Maximum Mean Discrepancy (MMD) loss, a robust non-parametric metric for comparing distributions. A key aspect of our method is that the target standard deviation  $\sigma^*$  is not fixed but is learned adaptively via a parameter  $\omega$  ( $\sigma^* = e^\omega$ ), allowing the model to determine the appropriate noise level for the data. The MMD is computed using a multi-bandwidth Radial Basis Function (RBF) kernel, defined as:

$$\kappa(a, b) = \sum_{j=1}^M \exp\left(-\frac{\|a - b\|^2}{2(B_j \sigma^*)^2}\right), \quad (2)$$

where  $\{B_j\}_{j=1}^M$  is a set of predefined bandwidth multipliers. To ensure the MMD metric is robust and sensitive to discrepancies at various scales, we employ a multi-bandwidth kernel. Guided by the median heuristic, we set the multipliers to  $\{0.1, 0.5, 1.0, 2.0, 5.0\}$ . The MMD loss then measures

the distance between the set of residual vectors  $R$  and samples  $S$  from the target Gaussian:

$$\begin{aligned} \mathcal{L}_{\text{MMD}} = & \frac{1}{|R|^2} \sum_{p_i, p_j \in R} \kappa(p_i, p_j) + \frac{1}{|S|^2} \sum_{q_i, q_j \in S} \kappa(q_i, q_j) \\ & - \frac{2}{|R||S|} \sum_{p_i \in R, q_j \in S} \kappa(p_i, q_j). \end{aligned} \quad (3)$$

Minimizing this loss drives the residuals towards a zero-mean Gaussian distribution, penalizing systematic biases and complex structures that could indicate overfitting.

**White Noise Regularization ( $\mathcal{L}_{\text{ACF}}$ ).** This loss penalizes significant temporal correlations by summing the squared autocorrelation coefficients ( $\rho_k$ ) over a set of lags  $N_{\text{lag}}$ . Based on the empirical observation that the most salient correlations typically manifest within early lags, we set  $N_{\text{lag}} = \{1, \dots, 10\}$  to strike a balance between regularization effectiveness and computational cost. The calculation is performed for each feature sequence within the batch, and the final loss is the average over all sequences:

$$\mathcal{L}_{\text{ACF}} = \sum_{k \in N_{\text{lag}}} \mathbb{E}_{b,d} [(\rho_{k,b,d})^2], \quad (4)$$

where  $\rho_{k,b,d}$  is the autocorrelation coefficient at lag  $k$  for the residual series  $R_{b,d} = (r_{b,1,d}, \dots, r_{b,L,d})$ . It is computed as:

$$\rho_{k,b,d} = \frac{\sum_{l=k+1}^L (r_{b,l,d} - \mu_{b,d})(r_{b,l-k,d} - \mu_{b,d})}{\sum_{l=1}^L (r_{b,l,d} - \mu_{b,d})^2}, \quad (5)$$

where  $\mu_{b,d}$  is the mean of the residual series  $R_{b,d}$ . Minimizing this term forces the model to produce residuals that are temporally independent.

**Final Objective with Automatic Weighting.** To combine these three loss components, we employ Automatic

Weighted Loss (AWL) (Kendall, Gal, and Cipolla 2018), a technique that dynamically balances the contribution of each loss term by introducing learnable weight parameters. This avoids manual tuning and leads to more stable training. The final objective is formulated as:

$$\mathcal{L}_{\text{Total}} = \mathcal{L}_{\text{AWL}}(\mathcal{L}_{\text{MSE}}, \mathcal{L}_{\text{MMD}}, \mathcal{L}_{\text{ACF}}). \quad (6)$$

Through this composite objective, we guide the model to not only reconstruct normal data accurately but also to generate residuals that are certifiably Gaussian and white, creating the ideal statistical foundation for our subsequent Kalman Smoothing Post-processor.

### Kalman Smoothing Post-processor

Reconstruction errors often yield noisy, unstable anomaly scores, degrading detection. We address this by framing the denoising task as a state estimation problem and applying a Kalman Filter followed by a RTS smoother (Rauch, Tung, and Striebel 1965). This approach is motivated by a foundational result in estimation theory: the Kalman Filter is a provably optimal linear estimator under the assumption that noise processes are zero-mean, uncorrelated (i.e., white), and Gaussian-distributed (Kalman 1960). Crucially, these are precisely the statistical properties our GWRN strategy is designed to enforce on the residuals, creating the ideal conditions for our post-processor to operate at its theoretical optimum.

We model the problem from a univariate perspective, treating the residual sequence of each feature channel independently. For notational generality, we express the state-space model in its standard matrix form. For a given channel, let the sequence of raw reconstruction residuals,  $r_t$ , serve as the noisy observation sequence for our model. We posit that this observed residual is a manifestation of a latent “true” anomaly state,  $s_t$ , corrupted by measurement noise. We assume a simple random walk for the state dynamics and a linear observation model, which captures the intuition that anomaly states often exhibit temporal persistence:

$$\begin{cases} s_t = F s_{t-1} + w_t, & w_t \sim \mathcal{N}(0, Q_p) \\ r_t = H s_t + v_t, & v_t \sim \mathcal{N}(0, R_m), \end{cases} \quad (7)$$

where  $F = I$  and  $H = I$  are the state transition and observation matrices. The process noise  $w_t$  and measurement noise  $v_t$  are assumed to be zero-mean Gaussian noise with covariances  $Q_p$  and  $R_m$ , respectively. The measurement noise covariance  $R_m$  is empirically estimated from the variance of residuals on the training set, and the process noise is set as  $Q_p = \lambda R_m$ . Here,  $\lambda$  serves as a hyperparameter that tunes the balance of the **Bias-Variance Tradeoff** across various backbones.

The estimation is performed via a two-pass procedure: a forward Kalman filter pass followed by a backward RTS smoother pass.

**Forward Pass: Kalman Filter.** The forward pass iteratively computes the filtered state estimate  $\hat{s}_{t|t}$  and its covariance  $P_{t|t}$  using all observations up to time  $t$ . For each time step, this involves two stages:

1. **Prediction Step:** The state and its covariance are projected forward based on the previous state estimate.

$$\begin{cases} \hat{s}_{t|t-1} = F \hat{s}_{t-1|t-1}, \\ P_{t|t-1} = F P_{t-1|t-1} F^T + Q_p. \end{cases} \quad (8)$$

2. **Update Step:** The prediction is corrected using the new measurement  $r_t$ . First, the Kalman Gain  $K_t$  is computed to balance the uncertainty of the prediction and the measurement.

$$\begin{cases} K_t = P_{t|t-1} H^T (H P_{t|t-1} H^T + R_m)^{-1}, \\ \hat{s}_{t|t} = \hat{s}_{t|t-1} + K_t (r_t - H \hat{s}_{t|t-1}), \\ P_{t|t} = (I - K_t H) P_{t|t-1}. \end{cases} \quad (9)$$

**Backward Pass: RTS Smoother.** After the forward pass completes, the backward pass refines these estimates by incorporating information from all future observations. This pass initializes with the final filtered estimate from the forward pass ( $\hat{s}_{t|t}, P_{t|t}$ ) and proceeds backward from  $t = T - 1$  to 0. At each step, it computes a smoother gain  $G_t$  that blends the filtered estimate with the smoothed future estimate:

$$G_t = P_{t|t} F^T (P_{t+1|t})^{-1}, \quad (10)$$

where  $P_{t+1|t}$  is the one-step predicted state covariance from the forward pass (Eq. 8). This gain is used to update the state estimate, correcting the filtered estimate based on subsequently observed data:

$$\hat{s}_{t|T} = \hat{s}_{t|t} + G_t (\hat{s}_{t+1|T} - \hat{s}_{t+1|t}). \quad (11)$$

The term  $(\hat{s}_{t+1|T} - \hat{s}_{t+1|t})$  in Eq. (11) represents the new information gained from future data, allowing the smoother to yield a globally optimal state estimate  $\hat{s}_{t|T}$  given the entire observation sequence.

Finally, since the latent state  $s_t$  represents the underlying anomaly magnitude (which should be near zero for normal data), the final, denoised anomaly score for time  $t$  is calculated as the squared value of its smoothed estimate:

$$\text{Anomaly Score}_t = (\hat{s}_{t|T})^2. \quad (12)$$

This process is applied in parallel to each channel, and the resulting scores are aggregated to produce highly stable anomaly score for each time point in the multivariate series.

## Experiments

### Experiments Settings

**Datasets and Evaluation Metrics.** We conduct experiments using four widely-used real-world time series anomaly detection datasets: MSL (Hundman et al. 2018), SMAP (Hundman et al. 2018), SWaT (Mathur and Tippenhauer 2016), PSM (Abdulaal, Liu, and Lancewicki 2021). These datasets represent diverse application domains, including service monitoring, space and earth exploration, and water treatment. More details can be found in Appendix.

To robustly evaluate time series anomaly detection, accounting for temporal context beyond traditional point-wise metrics, we employ two strategies. First, the point-adjustment strategy (Xu et al. 2018) deems a segment detected if any internal point is identified. Second, for a more

Datasets	SWaT						MSL						PSM					
	Vanilla			COGNOS			Vanilla			COGNOS			Vanilla			COGNOS		
Models	AP	AR	AF	AP	AR	AF	AP	AR	AF	AP	AR	AF	AP	AR	AF	AP	AR	AF
AnomalyT	<b>0.908</b>	0.345	0.425	0.880	<b>0.794</b>	<b>0.833</b>	0.873	0.378	0.522	<b>0.907</b>	<b>0.981</b>	<b>0.942</b>	<b>0.961</b>	0.561	0.675	0.941	<b>0.768</b>	<b>0.842</b>
Autoformer	<b>0.944</b>	0.329	0.399	0.916	<b>0.664</b>	<b>0.762</b>	0.870	0.441	0.572	<b>0.917</b>	<b>0.991</b>	<b>0.952</b>	<b>1.000</b>	0.464	0.576	0.915	<b>0.799</b>	<b>0.852</b>
Dlinear	0.810	0.663	0.716	<b>0.917</b>	<b>0.666</b>	<b>0.763</b>	0.831	0.456	0.580	<b>0.902</b>	<b>0.981</b>	<b>0.939</b>	<b>0.923</b>	0.665	0.763	0.887	<b>0.996</b>	<b>0.936</b>
FiLM	0.790	0.541	0.609	<b>0.879</b>	<b>0.989</b>	<b>0.931</b>	0.814	0.194	0.314	<b>0.878</b>	<b>0.951</b>	<b>0.912</b>	0.837	0.508	0.590	<b>0.920</b>	<b>0.996</b>	<b>0.956</b>
iTrans	0.834	0.664	0.722	<b>0.865</b>	<b>1.000</b>	<b>0.928</b>	0.844	0.426	0.551	<b>0.905</b>	<b>0.981</b>	<b>0.941</b>	<b>0.866</b>	0.616	0.711	0.884	<b>0.996</b>	<b>0.934</b>
LightTS	<b>0.836</b>	0.669	0.727	0.833	<b>0.797</b>	<b>0.814</b>	0.843	0.450	0.577	<b>0.929</b>	<b>1.000</b>	<b>0.963</b>	<b>0.890</b>	0.653	0.744	0.884	<b>0.995</b>	<b>0.934</b>
MICN	0.818	0.764	0.787	<b>0.896</b>	<b>1.000</b>	<b>0.945</b>	0.852	0.371	0.511	<b>0.908</b>	<b>0.981</b>	<b>0.942</b>	<b>0.957</b>	0.667	0.778	0.886	<b>0.998</b>	<b>0.937</b>
PatchTsT	0.823	0.507	0.593	<b>0.867</b>	<b>1.000</b>	<b>0.929</b>	0.844	0.456	0.575	<b>0.922</b>	<b>0.999</b>	<b>0.959</b>	<b>0.949</b>	0.624	0.737	0.894	<b>0.997</b>	<b>0.941</b>
Pyraformer	0.813	0.336	0.411	<b>0.899</b>	<b>0.693</b>	<b>0.776</b>	0.868	0.411	0.548	<b>0.923</b>	<b>1.000</b>	<b>0.960</b>	<b>0.940</b>	0.637	0.740	0.898	<b>0.825</b>	<b>0.860</b>
TimeMixer	0.878	0.499	0.599	<b>0.960</b>	<b>1.000</b>	<b>0.980</b>	0.828	0.458	0.581	<b>0.883</b>	<b>0.948</b>	<b>0.913</b>	<b>0.943</b>	0.635	0.743	0.901	<b>0.999</b>	<b>0.946</b>
TimesNet	0.828	0.681	0.734	<b>0.864</b>	<b>1.000</b>	<b>0.927</b>	0.855	0.444	0.571	<b>0.911</b>	<b>0.990</b>	<b>0.949</b>	<b>0.943</b>	0.757	0.833	0.895	<b>0.998</b>	<b>0.942</b>
Transformer	<b>0.918</b>	0.345	0.426	0.894	<b>0.809</b>	<b>0.847</b>	0.874	0.379	0.522	<b>0.917</b>	<b>0.989</b>	<b>0.952</b>	<b>0.974</b>	0.566	0.682	0.958	<b>0.767</b>	<b>0.846</b>
AVG	0.850	0.529	0.596	<b>0.889</b>	<b>0.868</b>	<b>0.869</b>	0.850	0.405	0.535	<b>0.908</b>	<b>0.982</b>	<b>0.944</b>	<b>0.932</b>	0.613	0.714	0.905	<b>0.928</b>	<b>0.910</b>

Table 1: Anomaly detection results across three datasets. Best results are highlighted in **bold**.

rigorous and shift-insensitive assessment, affiliation-based metrics (Huet, Navarro, and Rossi 2022) extend precision and recall by measuring temporal distance. We report Average Precision, Recall, and F-Score for both criteria to provide a comprehensive evaluation.

**Backbones.** To comprehensively evaluate our method, we integrate it with 12 different backbone models, encompassing various architectural paradigms, such as attention-based models: AnomalyTransformer (Xu et al. 2022), Autoformer (Wu et al. 2021), PatchTsT (Nie et al. 2023), Pyraformer (Liu et al. 2022b), Transformer (Vaswani et al. 2017), iTransformer (Liu et al. 2024); time-frequency fusion models: TimesNet (Wu et al. 2023), TimeMixer (Wang et al. 2024a), FiLM (Zhou et al. 2022); and CNN-MLP-based models: MICN (Wang et al. 2023), LightTS (Campos et al. 2023), DLinear (Zeng et al. 2023).

**Implementation Details.** We utilized the official implementations of each backbone model. To ensure a fair evaluation, we adhered to their original experimental and hyperparameter settings, while only tuning the Bias-Variance Tradeoff  $\lambda$ , the main hyperparameter details can be found in Appendix. All experiments were implemented using PyTorch on a single NVIDIA RTX 4090 GPU.

## Experimental Results

**Main Results.** We present a comprehensive evaluation of our proposed method in Table 1 and Table 2. The results clearly indicate that our method provides a substantial performance advantage over the conventional MSE-based reconstruction and inference baseline. Across all tested model architectures and benchmark datasets, our approach yields an **average F-score uplift of 57.9% across 12 backbones**.

This improvement is observed consistently. Among the backbones, FiLM benefits the most, achieving a remarkable

Datasets	SMAP					
	Vanilla			COGNOS		
Models	AP	AR	AF	AP	AR	AF
AnomalyT	<b>0.835</b>	0.367	0.497	0.817	<b>0.719</b>	<b>0.747</b>
Autoformer	0.890	0.416	0.545	<b>0.913</b>	<b>0.953</b>	<b>0.931</b>
Dlinear	<b>0.894</b>	0.354	0.488	0.850	<b>0.733</b>	<b>0.773</b>
FiLM	<b>0.875</b>	0.304	0.420	0.799	<b>0.708</b>	<b>0.739</b>
iTrans	0.822	0.316	0.437	<b>0.860</b>	<b>0.778</b>	<b>0.811</b>
LightTS	<b>0.879</b>	0.353	0.486	0.841	<b>0.721</b>	<b>0.761</b>
MICN	<b>0.848</b>	0.337	0.465	0.806	<b>0.676</b>	<b>0.721</b>
PatchTsT	0.869	0.377	0.511	<b>0.886</b>	<b>0.832</b>	<b>0.852</b>
Pyraformer	0.853	0.362	0.491	<b>0.911</b>	<b>0.937</b>	<b>0.923</b>
TimeMixer	0.893	0.395	0.534	<b>0.904</b>	<b>0.892</b>	<b>0.896</b>
TimesNet	0.875	0.349	0.480	<b>0.906</b>	<b>0.874</b>	<b>0.886</b>
Transformer	0.854	0.381	0.515	<b>0.887</b>	<b>0.834</b>	<b>0.854</b>
AVG	<b>0.866</b>	0.359	0.489	0.865	<b>0.805</b>	<b>0.824</b>

Table 2: Anomaly Detection results of SMAP dataset. The table reports Average Precision (AP), Average Recall (AR), and Average F-Score (AF). Best results are highlighted in **bold**. The full experiment results and more details can be found in Appendix.

**95.4%** improvement on F-Score, in contrast, DLinear registers the smallest yet still considerable gain of **37.4%**. Other models also show significant gains: attention-based models improve by an average of **62.5%**, time-frequency fusion models by **50.7%**, and CNN-MLP models by **42.6%**. Collectively, these findings provide compelling evidence for not only the effectiveness of our method but also its impressive ability to generalize to a wide range of model architectures.

Dataset	MSL & PSM											
	COGNOS			$w$ /GWRN+MA			$w$ /GWRN+LP			$w$ /oGWRN+KS		
Models	AP	AR	AF	AP	AR	AF	AP	AR	AF	AP	AR	AF
AnomalyT	<b>0.924</b>	<b>0.874</b>	<b>0.892</b>	<u>0.920</u>	<u>0.815</u>	<u>0.850</u>	0.899	0.767	0.817	0.902	0.730	0.779
Autoformer	<b>0.916</b>	<b>0.895</b>	<b>0.902</b>	0.892	<u>0.847</u>	<u>0.862</u>	<u>0.914</u>	0.785	0.833	0.884	0.788	0.814
Dlinear	<u>0.894</u>	<u>0.988</u>	<u>0.938</u>	0.868	0.921	0.891	0.887	0.915	0.899	<b>0.910</b>	<b>0.995</b>	<b>0.950</b>
FiLM	<b>0.899</b>	<b>0.973</b>	<b>0.934</b>	0.850	0.841	0.840	<u>0.858</u>	0.849	0.849	0.846	<u>0.904</u>	<u>0.869</u>
iTrans	<u>0.894</u>	<b>0.988</b>	<b>0.937</b>	0.865	0.925	0.891	0.891	0.923	0.905	<b>0.905</b>	<u>0.968</u>	<u>0.935</u>
LightTS	<u>0.906</u>	<b>0.998</b>	<b>0.949</b>	0.886	0.952	0.916	0.888	0.913	0.899	<b>0.910</b>	<u>0.992</u>	<u>0.948</u>
MICN	<b>0.897</b>	<b>0.990</b>	<b>0.940</b>	0.877	<u>0.959</u>	0.913	0.851	0.845	0.843	<u>0.884</u>	0.952	<u>0.914</u>
PatchTsT	<b>0.908</b>	<b>0.998</b>	<b>0.950</b>	0.877	0.928	0.899	<u>0.890</u>	0.906	0.896	<b>0.908</b>	<u>0.989</u>	<u>0.946</u>
Pyraformer	<b>0.910</b>	<b>0.913</b>	<b>0.910</b>	0.875	<u>0.880</u>	<u>0.876</u>	0.890	0.810	0.842	<u>0.902</u>	0.694	0.731
TimeMixer	<b>0.892</b>	<b>0.973</b>	<b>0.929</b>	0.859	0.892	0.873	0.850	0.785	0.804	<u>0.875</u>	<u>0.950</u>	<u>0.909</u>
TimesNet	<u>0.903</u>	<b>0.994</b>	<b>0.945</b>	0.891	0.956	0.920	0.894	0.865	0.877	<b>0.911</b>	<u>0.970</u>	<u>0.939</u>
Transformer	<b>0.938</b>	<b>0.878</b>	<b>0.899</b>	0.913	0.814	0.850	<u>0.915</u>	0.769	0.821	0.898	0.713	0.763
<b>AVG</b>	<b>0.907</b>	<b>0.955</b>	<b>0.927</b>	0.881	<u>0.894</u>	<u>0.882</u>	0.886	0.844	0.857	<u>0.895</u>	0.887	0.875

Table 3: Ablation Study of COGNOS Components and Filtering Methods. The best results are highlighted in **bold**, and the second-best are underlined. The full experiment results and more details can be found in the Appendix.

**Ablation Studies.** We evaluated the contribution of the synergy in COGNOS on the MSL and PSM datasets, with average results presented in Table 3.

**Kalman Smoothing Post-processor:** We first validate our Kalman Smoother (KS) by replacing it with two common filtering alternatives: a heuristic moving average (MA) and a classic low-pass filter (LP). The performance degradation observed with both alternatives underscores the superiority of our statistically-grounded approach. While heuristic filters can reduce noise, the Kalman Smoother is theoretically optimal because our GWRN creates the ideal Gaussian white noise conditions under which it can effectively separate the true anomaly signal from random fluctuations.

**Gaussian-White Noise Regularization:** Removing GWRN degrades performance consistency, underscoring its foundational role in compelling statistically random residuals to prevent overfitting to spurious patterns and ensure a robust normalcy representation. The complete COGNOS’s superior performance confirms the powerful synergy between our regularization and smoothing components.

**Comparison with Other Methods.** To contextualize the performance of COGNOS, we benchmark it against two pivotal approaches: the standard MSE-based training, and Floss (Yang et al. 2023a), which operates by enforcing periodic consistency in the latent representation space.

As demonstrated in Table 4, COGNOS significantly outperforms both the baseline and Floss across all datasets and backbone architectures. The superiority over the MSE is expected. More importantly, its advantage over Floss highlights a key difference: while Floss refines the latent space, COGNOS adopts a more direct approach by regularizing the final output residuals. This strategy not only yields a cleaner anomaly signal but also creates optimal preconditions for our subsequent smoothing stage, explaining the substantial performance gains.

Models		TimesNet			Transformer		
Datasets	Methods	MSE	FLoss	Ours	MSE	FLoss	Ours
MSL	AP	0.855	<u>0.857</u>	<b>0.911</b>	<u>0.874</u>	0.861	<b>0.917</b>
	AR	<u>0.444</u>	0.372	<b>0.990</b>	0.379	<u>0.405</u>	<b>0.989</b>
	AF	<u>0.571</u>	0.511	<b>0.949</b>	0.522	<u>0.543</u>	<b>0.952</b>
PSM	AP	<b>0.943</b>	<u>0.913</u>	0.895	<b>0.974</b>	<u>0.972</u>	0.958
	AR	<u>0.757</u>	0.638	<b>0.998</b>	<u>0.566</u>	0.543	<b>0.767</b>
	AF	<u>0.833</u>	0.743	<b>0.942</b>	<u>0.682</u>	0.666	<b>0.846</b>
SMAP	AP	<u>0.875</u>	0.843	<b>0.906</b>	0.854	<u>0.862</u>	<b>0.887</b>
	AR	0.349	<u>0.371</u>	<b>0.874</b>	0.381	<u>0.415</u>	<b>0.834</b>
	AF	0.480	<u>0.502</u>	<b>0.886</b>	0.515	<u>0.552</u>	<b>0.854</b>
SWaT	AP	<u>0.828</u>	0.782	<b>0.864</b>	<u>0.918</u>	<b>0.924</b>	0.894
	AR	<u>0.681</u>	0.484	<b>1.000</b>	<u>0.345</u>	0.329	<b>0.809</b>
	AF	<u>0.734</u>	0.565	<b>0.927</b>	<u>0.426</u>	0.398	<b>0.847</b>

Table 4: Comparison between COGNOS and other methods. Best results are in **bold**, and second-best are underlined.

**Visualization.** Fig. 14 visually confirms COGNOS’s effectiveness. While the vanilla method produces anomaly scores plagued by high-frequency noise and spurious spikes, COGNOS generates a remarkably stable signal. This suppression of erratic fluctuations significantly enhances the signal-to-noise ratio, clearly delineating true anomalous events.

This improvement stems directly from our regularization strategy, as evidenced in Fig. 11. We analyze the residuals of the FiLM backbone on the PSM dataset. The Q-Q and ACF plots reveal that residuals from the vanilla model exhibit strong temporal autocorrelation and a clear deviation from a

Gaussian distribution. After applying COGNOS, the residuals are demonstrably closer to the ideal of Gaussian white noise: the autocorrelation is substantially suppressed across all lags, and the Q-Q plot shows a much tighter alignment with the theoretical quantiles (variance reduced from  $10^6$  to  $10^2$ ). This confirms that our regularization strategy successfully engineers the desired statistical properties in the residuals, which is the foundational reason for the cleaner, more reliable anomaly scores. Further visualizations for other models are available in the Appendix.

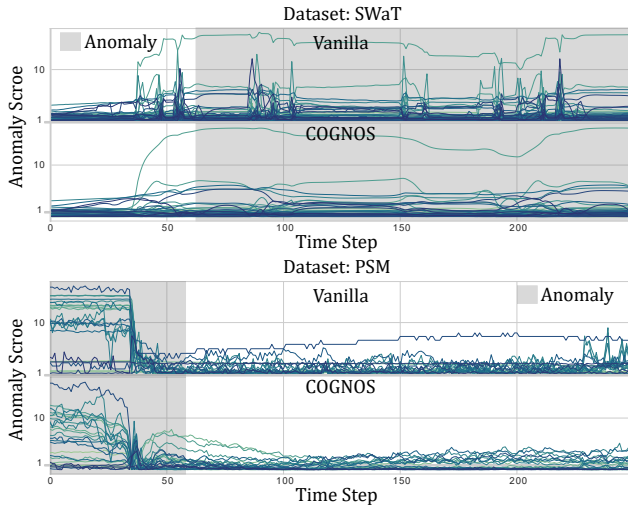


Figure 3: Qualitative comparison of anomaly scores on the SWaT and PSM datasets using a Transformer backbone. The vanilla MSE baseline produces noisy scores, whereas COGNOS yields stable scores with a clear separation between normal and anomalous periods.

**Hyperparameter Sensitivity.** Our framework introduces a single hyperparameter, the Bias-Variance Tradeoff ( $\lambda$ ), which adjusts the sensitivity of the Kalman Smoother. We evaluated its impact on four diverse backbones (Fig. 5) within a range of  $\lambda \in \{0.1, 0.3, 0.5, 0.7, 1.0, 3.0, 5.0, 10.0\}$ . Across the datasets, performance remained consistently high over a wide range of  $\lambda$  values. While results on MSL suggest that excessively low values can slightly degrade performance by over-smoothing subtle anomalies, any variation from tuning  $\lambda$  is marginal compared to the substantial improvements delivered by COGNOS.

## Conclusion

In this work, we propose COGNOS, which address a core weakness of reconstruction-based time series anomaly detection: the statistically flawed and noisy anomaly scores produced by standard MSE-based training. Experiments show COGNOS is model-agnostic and highly effective, delivering a significant performance improvement. The results confirm this gain stems from the powerful synergy between our regularization and smoothing components. Our work demonstrates that directly regularizing output statistics is a

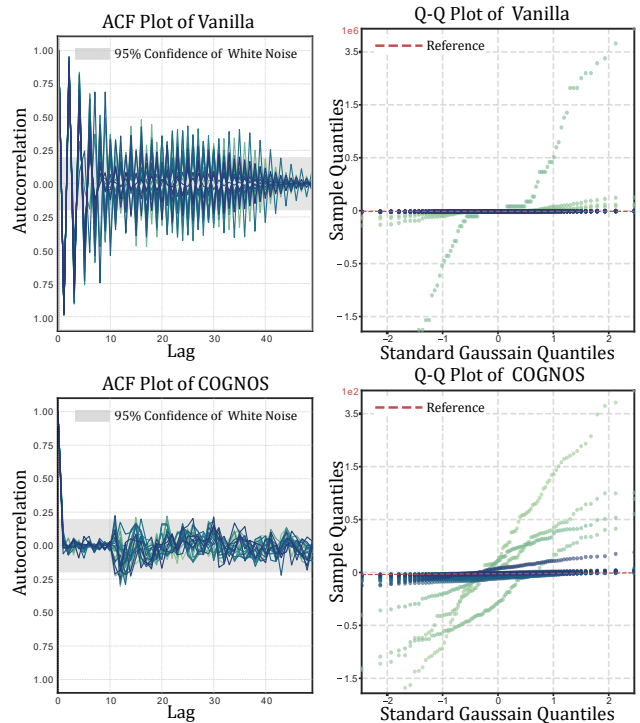


Figure 4: Visual analysis of reconstruction residuals for the FiLM backbone on the PSM dataset. Top row: Residuals from the vanilla method show strong autocorrelation (ACF) and non-Gaussianity (Q-Q plot). Bottom row: COGNOS successfully regularizes the residuals, suppressing autocorrelation and enforcing a distribution much closer to Gaussian white noise.

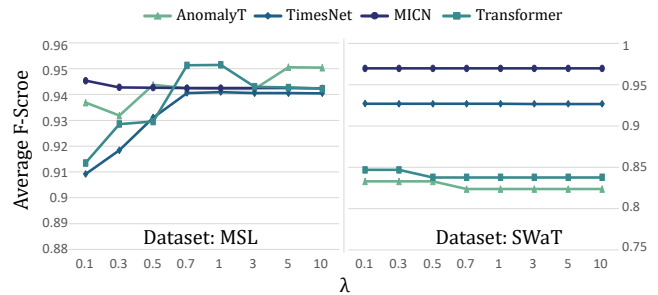


Figure 5: The impact of the Bias-Variance Tradeoff  $\lambda$  on four backbones across the MSL and SWaT datasets.

potent strategy, presenting a new direction beyond conventional architectural or representation-focused improvements. Future work may include exploring multivariate extensions and scaling to Video Anomaly Detection.

## References

Abdulaal, A.; Liu, Z.; and Lanczewicki, T. 2021. Practical approach to asynchronous multivariate time series anomaly detection and localization. In *Proceedings of the 27th ACM*

- SIGKDD conference on knowledge discovery & data mining*, 2485–2494.
- Campos, D.; Zhang, M.; Yang, B.; Kieu, T.; Guo, C.; and Jensen, C. S. 2023. Lightts: Lightweight time series classification with adaptive ensemble distillation. *Proceedings of the ACM on Management of Data*, 1(2): 1–27.
- Darban, Z. Z.; Webb, G. I.; Pan, S.; Aggarwal, C. C.; and Salehi, M. 2025. CARLA: Self-supervised contrastive representation learning for time series anomaly detection. *Pattern Recognition*, 157: 110874.
- Eldele, E.; Ragab, M.; Chen, Z.; Wu, M.; Kwok, C. K.; Li, X.; and Guan, C. 2021. Time-Series Representation Learning via Temporal and Contextual Contrasting. In *Proceedings of the Thirtieth International Joint Conference on Artificial Intelligence*, 2352–2359. International Joint Conferences on Artificial Intelligence Organization.
- Franceschi, J.-Y.; Dieuleveut, A.; and Jaggi, M. 2019. Un-supervised scalable representation learning for multivariate time series. *Advances in Neural Information Processing Systems*, 32.
- Huang, X.; Chen, W.; Hu, B.; and Mao, Z. 2025. Graph Mixture of Experts and Memory-augmented Routers for Multivariate Time Series Anomaly Detection. *Proceedings of the AAAI Conference on Artificial Intelligence*, 39(16): 17476–17484.
- Huang, X.; Zhang, F.; Wang, R.; Lin, X.; Liu, H.; and Fan, H. 2023. KalmanAE: Deep embedding optimized Kalman filter for time series anomaly detection. *IEEE Transactions on Instrumentation and Measurement*, 72: 1–11.
- Huet, A.; Navarro, J. M.; and Rossi, D. 2022. Local Evaluation of Time Series Anomaly Detection Algorithms. In *Proceedings of the 28th ACM SIGKDD Conference on Knowledge Discovery and Data Mining*, KDD '22, 635–645. New York, NY, USA: Association for Computing Machinery. ISBN 9781450393850.
- Hundman, K.; Constantinou, V.; Laporte, C.; Colwell, I.; and Soderstrom, T. 2018. Detecting spacecraft anomalies using lstms and nonparametric dynamic thresholding. In *Proceedings of the 24th ACM SIGKDD international conference on knowledge discovery & data mining*, 387–395.
- Kalman, R. E. 1960. A new approach to linear filtering and prediction problems.
- Kendall, A.; Gal, Y.; and Cipolla, R. 2018. Multi-Task Learning Using Uncertainty to Weigh Losses for Scene Geometry and Semantics. In *Proceedings of the IEEE Conference on Computer Vision and Pattern Recognition (CVPR)*.
- Kieu, T.; Yang, B.; Guo, C.; Jensen, C. S.; Zhao, Y.; Huang, F.; and Zheng, K. 2022. Robust and explainable autoencoders for unsupervised time series outlier detection. In *2022 IEEE 38th International conference on data engineering (ICDE)*, 3038–3050. IEEE.
- Liu, F.; Zhou, X.; Cao, J.; Wang, Z.; Wang, T.; Wang, H.; and Zhang, Y. 2022a. Anomaly Detection in Quasi-Periodic Time Series Based on Automatic Data Segmentation and Attentional LSTM-CNN. *IEEE Transactions on Knowledge and Data Engineering*, 34(6): 2626–2640.
- Liu, S.; Yu, H.; Liao, C.; Li, J.; Lin, W.; Liu, A. X.; and Dustdar, S. 2022b. Pyraformer: Low-Complexity Pyramidal Attention for Long-Range Time Series Modeling and Forecasting. In *The Tenth International Conference on Learning Representations*.
- Liu, Y.; Hu, T.; Zhang, H.; Wu, H.; Wang, S.; Ma, L.; and Long, M. 2024. iTransformer: Inverted Transformers Are Effective for Time Series Forecasting. In *The Twelfth International Conference on Learning Representations*.
- Ma, M.; Fu, L.; Zhai, Z.; and Sun, R.-B. 2024. Transformer based Kalman Filter with EM algorithm for time series prediction and anomaly detection of complex systems. *Measurement*, 229: 114378.
- Mathur, A. P.; and Tippenhauer, N. O. 2016. SWaT: A water treatment testbed for research and training on ICS security. In *2016 international workshop on cyber-physical systems for smart water networks (CySWater)*, 31–36. IEEE.
- Nie, Y.; Nguyen, N. H.; Sinthong, P.; and Kalagnanam, J. 2023. A Time Series is Worth 64 Words: Long-term Forecasting with Transformers. In *The Eleventh International Conference on Learning Representations*.
- Rauch, H. E.; Tung, F.; and Striebel, C. T. 1965. Maximum likelihood estimates of linear dynamic systems. *AIAA Journal*, 3(8): 1445–1450.
- Tonekaboni, S.; Eytan, D.; and Goldenberg, A. 2021. Un-supervised Representation Learning for Time Series with Temporal Neighborhood Coding. In *The Ninth International Conference on Learning Representations*.
- Vaswani, A.; Shazeer, N.; Parmar, N.; Uszkoreit, J.; Jones, L.; Gomez, A. N.; Kaiser, Ł.; and Polosukhin, I. 2017. Attention is all you need. *Advances in Neural Information Processing Systems*, 30.
- Wang, H.; Peng, J.; Huang, F.; Wang, J.; Chen, J.; and Xiao, Y. 2023. Micn: Multi-scale local and global context modeling for long-term series forecasting. In *The Eleventh International Conference on Learning Representations*.
- Wang, S.; Wu, H.; Shi, X.; Hu, T.; Luo, H.; Ma, L.; Zhang, J. Y.; and ZHOU, J. 2024a. TimeMixer: Decomposable Multiscale Mixing for Time Series Forecasting. In *The Twelfth International Conference on Learning Representations*.
- Wang, Y.; Wu, H.; Dong, J.; Liu, Y.; Long, M.; and Wang, J. 2024b. Deep Time Series Models: A Comprehensive Survey and Benchmark.
- Wu, H.; Hu, T.; Liu, Y.; Zhou, H.; Wang, J.; and Long, M. 2023. TimesNet: Temporal 2D-Variation Modeling for General Time Series Analysis. In *The Eleventh International Conference on Learning Representations*.
- Wu, H.; Xu, J.; Wang, J.; and Long, M. 2021. Autoformer: Decomposition transformers with auto-correlation for long-term series forecasting. *Advances in Neural Information Processing Systems*, 34: 22419–22430.
- Wu, X.; Qiu, X.; Li, Z.; Wang, Y.; Hu, J.; Guo, C.; Xiong, H.; and Yang, B. 2025. CATCH: Channel-Aware Multivariate Time Series Anomaly Detection via Frequency Patching. In *The Thirteenth International Conference on Learning Representations*.

Xu, H.; Chen, W.; Zhao, N.; Li, Z.; Bu, J.; Li, Z.; Liu, Y.; Zhao, Y.; Pei, D.; Feng, Y.; Chen, J.; Wang, Z.; and Qiao, H. 2018. Unsupervised Anomaly Detection via Variational Auto-Encoder for Seasonal KPIs in Web Applications. In *Proceedings of the 2018 World Wide Web Conference, WWW '18*, 187–196. Republic and Canton of Geneva, CHE: International World Wide Web Conferences Steering Committee. ISBN 9781450356398.

Xu, J.; Wu, H.; Wang, J.; and Long, M. 2022. Anomaly Transformer: Time Series Anomaly Detection with Association Discrepancy. In *The Tenth International Conference on Learning Representations*.

Yang, C.; Chen, X.; Sun, L.; Yang, H.; and Wu, Y. 2023a. Enhancing Representation Learning for Periodic Time Series with Floss: A Frequency Domain Regularization Approach. *CoRR*, abs/2308.01011.

Yang, Y.; Zhang, C.; Zhou, T.; Wen, Q.; and Sun, L. 2023b. DCdetector: Dual Attention Contrastive Representation Learning for Time Series Anomaly Detection. In *Proceedings of the 29th ACM SIGKDD Conference on Knowledge Discovery and Data Mining, KDD '23*, 3033–3045. New York, NY, USA: Association for Computing Machinery. ISBN 9798400701030.

Yao, Y.; Ma, J.; Feng, S.; and Ye, Y. 2024. SVD-AE: An asymmetric autoencoder with SVD regularization for multivariate time series anomaly detection. *Neural Networks*, 170: 535–547.

Yu, J.; Gao, X.; Li, B.; Zhai, F.; Lu, J.; Xue, B.; Fu, S.; and Xiao, C. 2024. A filter-augmented auto-encoder with learnable normalization for robust multivariate time series anomaly detection. *Neural networks*, 170: 478–493.

Yue, Z.; Wang, Y.; Duan, J.; Yang, T.; Huang, C.; Tong, Y.; and Xu, B. 2022. TS2Vec: Towards Universal Representation of Time Series. *Proceedings of the AAAI Conference on Artificial Intelligence*, 36(8): 8980–8987.

Zamanzadeh Darban, Z.; Webb, G. I.; Pan, S.; Aggarwal, C.; and Salehi, M. 2024. Deep learning for time series anomaly detection: A survey. *ACM Computing Surveys*, 57(1): 1–42.

Zeng, A.; Chen, M.; Zhang, L.; and Xu, Q. 2023. Are Transformers Effective for Time Series Forecasting? *Proceedings of the AAAI Conference on Artificial Intelligence*, 37(9): 11121–11128.

Zhou, T.; Ma, Z.; Wen, Q.; Sun, L.; Yao, T.; Yin, W.; Jin, R.; et al. 2022. Film: Frequency improved legendre memory model for long-term time series forecasting. *Advances in Neural Information Processing Systems*, 35: 12677–12690.

## Appendix

### Dataset Details

The the datasets used in the experiments are as follows, details are in Table 5:

- **MSL & SMAP** utilize expert-labeled Incident Surprise, Anomaly (ISA) reports from two operational domains: the Mars Science Laboratory (MSL) rover Curiosity and the Soil Moisture Active Passive (SMAP) satellite. These reports constitute canonical post-launch documentation of unexpected events that may jeopardize spacecraft health, serving as authoritative ground-truth data for anomaly-driven risk assessment. The objective is to leverage these curated corpora to advance data-driven methods for operational risk identification in robotic space missions.
- **PSM (Pooled Server Metrics)** is a publicly released, anonymized dataset derived from internal monitoring traces of multiple application-server nodes at eBay. Its primary research purpose is to supply a large-scale, real-world resource-usage corpus for the development and evaluation of anomaly-detection methodologies in distributed production environments.
- **SWaT (Secure Water Treatment)** is a purpose-built, small-scale yet fully operational water-treatment testbed designed to mirror the physical processes and control architectures of contemporary municipal plants. Jointly specified with Singapore’s Public Utility Board and realized by an industrial vendor, the facility serves as a realistic cyber-physical research platform. Its primary scientific objective is to systematically investigate cyber-attack mechanisms and plant-level responses, and to experimentally validate novel, especially physics-based, countermeasures.

Table 5: Dataset Details

Dataset	MSL	SMAP	SWaT	PSM
Channel Dim	55	25	51	25
Train Size	44,653	108,146	396,000	105,984
Validation Size	11,664	27,037	99,000	26,497
Test Size	73,729	427,617	449,919	87,841
Category	Spacecraft	Infrastructure	Server Machine	

### Backbone Hyperparameters

The backbone hyperparameters used in the experiments are detailed in Table 6. To ensure a fair and rigorous comparison, we adhered to the original hyperparameter settings specified in the official open-source implementations for each backbone model. The primary hyperparameter introduced by our framework is  $\lambda$ , which governs the bias-variance tradeoff in the Kalman Smoother. We made a principled choice for  $\lambda$  based on the characteristics of

each dataset. For datasets characterized by numerous short-duration anomaly segments (e.g., MSL), we set a higher  $\lambda$  (e.g.,  $\lambda = 1.0$ ) to balance denoising with preserving sensitivity to brief, transient events. Conversely, for datasets with predominantly long-duration anomalies (e.g., SWaT), a lower  $\lambda$  (e.g.,  $\lambda = 0.1$ ) was favored to produce a more heavily smoothed and stable output, effectively capturing the sustained nature of these anomalies.

Table 6: Hyperparameters Configurations

Miscellaneous Configurations									
Datasets	Hyper-parameter					Traning Process			
	Series Length	$d$ Model	$d$ MLP	Layers	Top k	$\lambda$	LR <sup>1</sup>	Batch Size	Epochs
MSL									
SMAP									
PSM						1			10
SWaT	100	128	128	3	3	0.1	$10^{-4}$	128	3
Model Specific Hyper-parameter									
Datasets	Model								
	TimesNet			TimeMixer					
	$d$ Model	$d$ MLP	Down Sampling Layers	Down Sampling Window	$d$ Model	$d$ MLP			
MSL									
SMAP									
PSM									
SWaT	8	16	3		2		16		32

### Visualizations

**Effect on GWNRR.** To provide a comprehensive evaluation of our GWNRR strategy’s effectiveness, we present visualizations of the reconstruction residuals for several backbones on the PSM and SMAP datasets. For each set of plots, we analyze a randomly sampled sequence of normal data from the test set, with a length corresponding to the backbone’s native input size, to validate the properties of the residuals.

The visualizations clearly demonstrate that GWNRR substantially reduces the temporal correlation in the residuals compared to the vanilla MSE-trained models. This effect is formally evaluated by examining whether the autocorrelation coefficients fall within the standard 95% confidence interval for white noise. For a sequence of length  $N$ , this interval is defined as:

$$\left[-\frac{z_{\alpha/2}}{\sqrt{N}}, \frac{z_{\alpha/2}}{\sqrt{N}}\right].$$

In this case, the interval is  $[-0.196, 0.196]$ . In the ACF plots (e.g., Figures 1, 3, 6), the coefficients produced by our method are markedly diminished and consistently fall within these bounds, providing strong evidence that the temporal dependencies have been successfully modeled.

Regarding Gaussianity, the Q-Q plots reveal two key improvements. First, a significant reduction in the variance of

<sup>1</sup>Initial Learning Rate

the residuals is observed across all backbones, with the overall variance typically reduced by at least an order of magnitude (e.g., Figures 1, 2, 4, 5, 6). Second, the residuals are better centered around zero, indicating a reduction in systematic bias (Figures 1, 6), and the linearity of the points in the Q-Q plots is also visibly improved, confirming that the residual distribution more closely approximates a Gaussian distribution (Figures 2, 5, 6).

**Anomaly Scores.** To provide further qualitative evidence, we present anomaly score sequences from various datasets and backbones. Each visualization displays a randomly sampled sequence of length 250 from the test set that includes anomalous points, allowing for a direct comparison of the anomaly scores before and after applying COGNOS. As observed in Figures 7 and 9, COGNOS effectively suppresses the erratic fluctuations and spurious spikes present in non-anomalous regions, thereby enhancing the signal of true anomalous deviations. Similarly, Figure 8 illustrates that the score becomes markedly more stable, capable of sustaining a high magnitude throughout the duration of an anomaly.

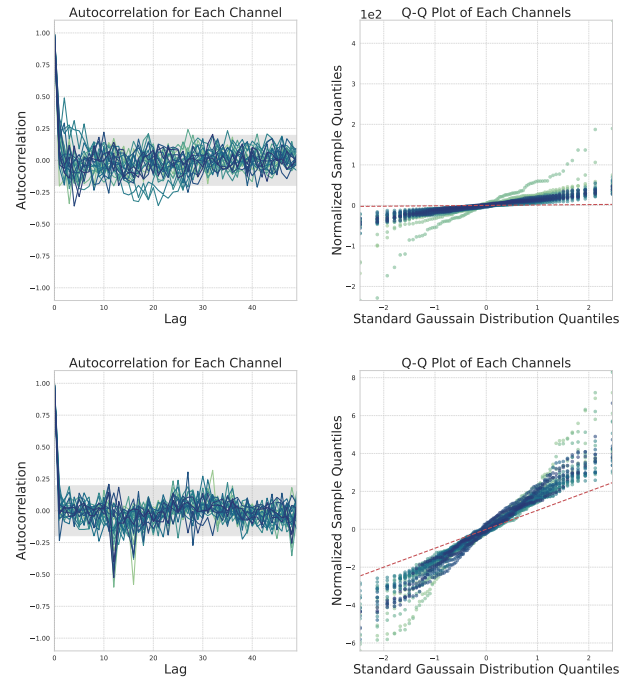


Figure 7: Visual analysis on the PSM dataset using MICN. Top row: vanilla method. Bottom row: COGNOS

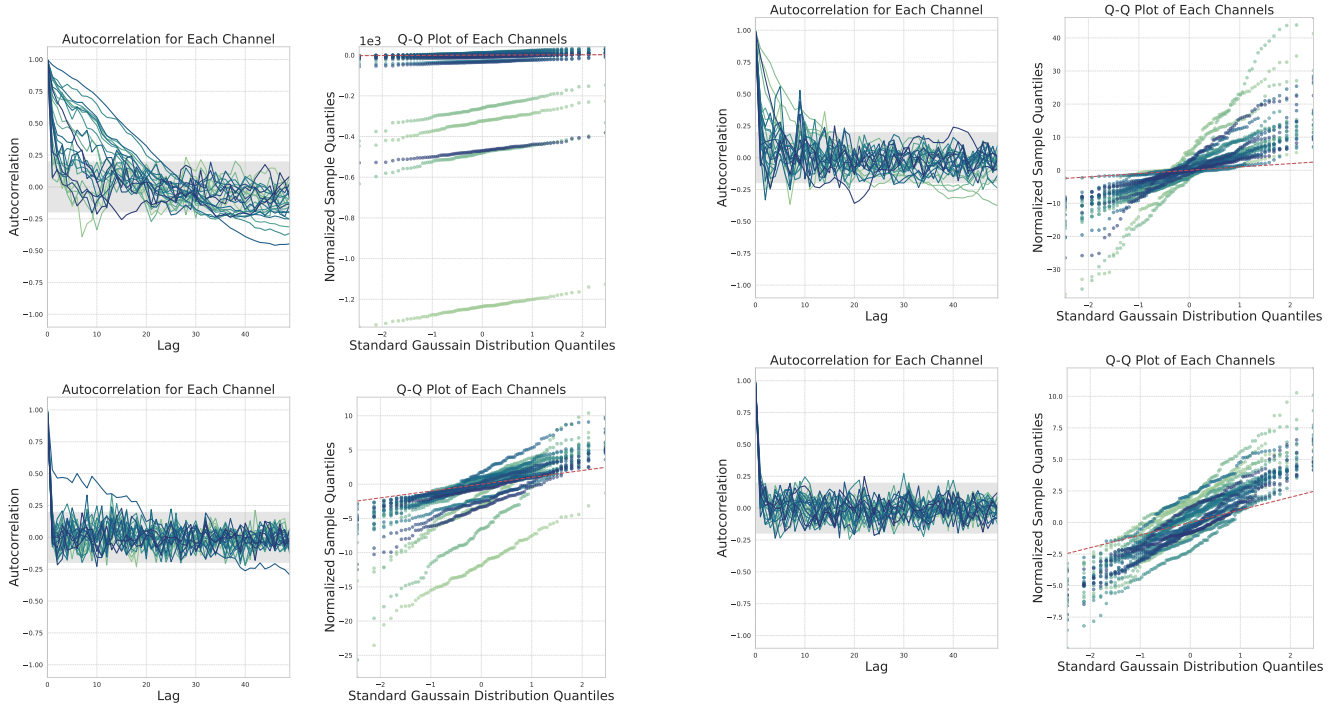


Figure 6: Visual analysis on the PSM dataset using Autoformer. Top row: vanilla method. Bottom row: COGNOS

Figure 8: Visual analysis on the PSM dataset using Pyraformer. Top row: vanilla method. Bottom row: COGNOS

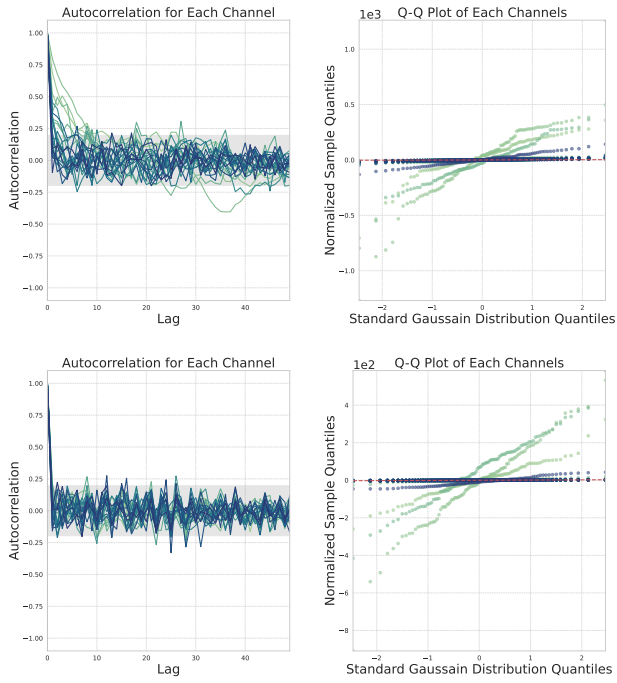


Figure 9: Visual analysis on the PSM dataset using TimesNet. Top row: vanilla method. Bottom row: COGNOS

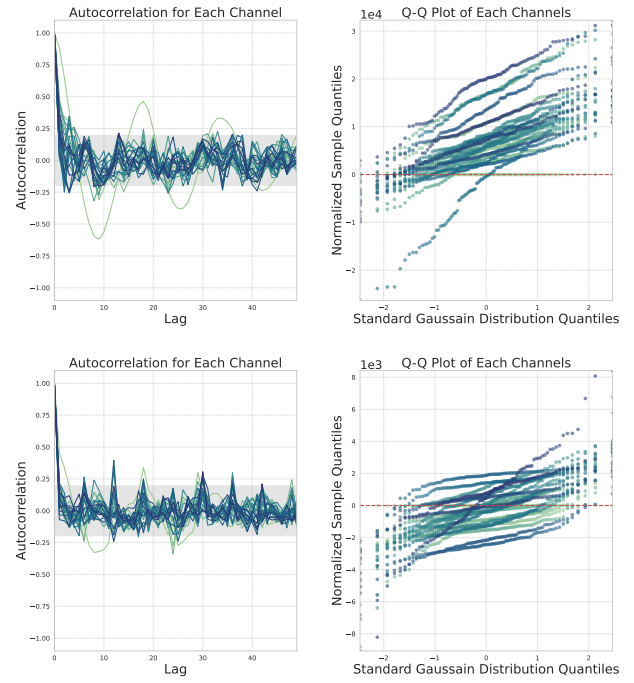


Figure 11: Visual analysis on the SMAP dataset using TimesNet. Top row: vanilla method. Bottom row: COGNOS

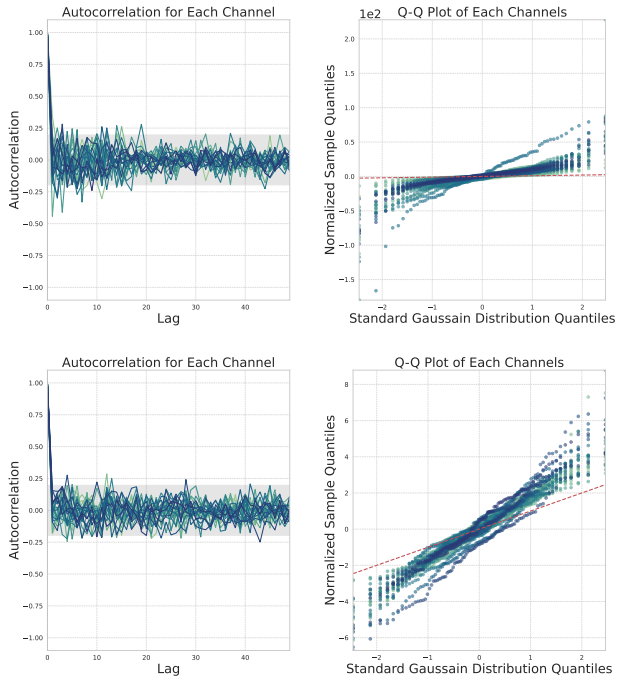


Figure 10: Visual analysis on the SMAP dataset using Transformer. Top row: vanilla method. Bottom row: COGNOS

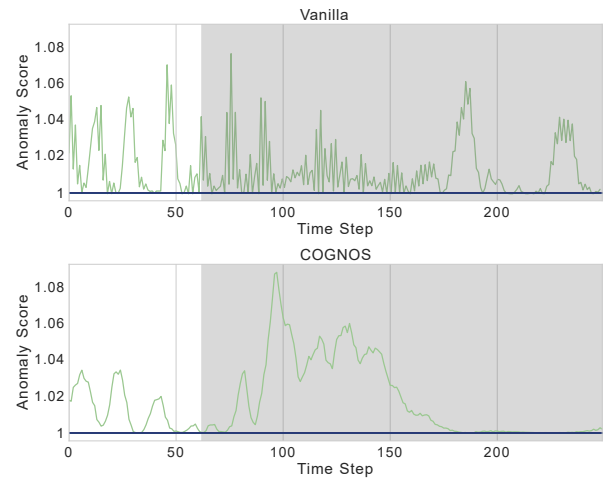


Figure 12: Comparison of anomaly scores on SMAP using FiLM.

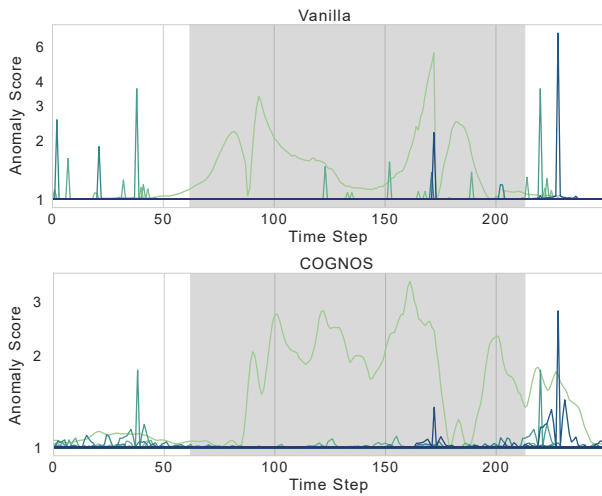


Figure 13: Qualitative comparison of anomaly scores on MSL using PatchTST.

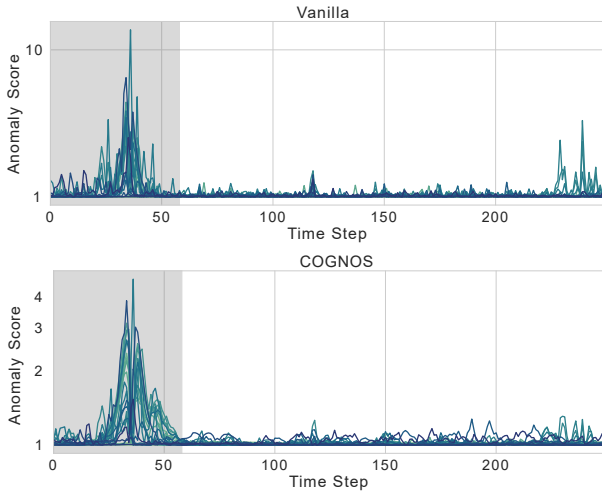


Figure 14: Qualitative comparison of anomaly scores on PSM using LightTS.

## Detailed Experiments

In this study, we evaluated performance on an AMD EPYC 7002 CPU with 48 GB of RAM, complemented by an NVIDIA RTX 4090 GPU equipped with 24 GB of VRAM. The source code was developed using Python 3.10 and PyTorch 2.3.0, and executed on an Ubuntu 22.04 operating system with CUDA 12.1 support. To ensure reproducibility, we fixed the random seed at 2021 across all experiments.

**Ablation Studies.** We present a comprehensive ablation study to dissect the contributions of COGNOS’s key components. This includes evaluations of the full COGNOS framework, comparisons with alternative filtering techniques (i.e., GWNr combined with moving average (MA) and low-pass (LP) filters), substitution of GWNr with standard MSE training (w/o GWNr + KS), removal of the filtering step while directly using MSE as the anomaly score (w/ GWNr + w/o Filter), and the vanilla baseline employing MSE for both training and anomaly scoring (w/o GWNr + w/o Filter). As evidenced in Tables 7, 8, 9, and 10, along with Figures 15 and 16, COGNOS consistently achieves superior and stable performance across diverse models and datasets.

**Main Results.** To assess performance, we employ evaluation metrics that surpass traditional point-wise measures in robustness. Conventional precision and recall often prove inadequate for time series data, as they overlook the temporal context inherent in anomalies. A widely adopted practical solution is the point-adjustment strategy (Xu et al. 2018), which considers an entire anomalous segment as detected if any point within it is correctly identified. To further enhance rigor and theoretical grounding, we incorporate the recently proposed affiliation-based metrics (Huet, Navarro, and Rossi 2022). This approach extends precision and recall by quantifying temporal distances between ground truth and predictions, thereby reducing sensitivity to minor temporal shifts and improving interpretability. Specifically, we compute precision (P), recall (R), and F-score (F) using the Adjusted metrics<sup>2</sup> and Affiliation metrics<sup>3</sup>. Detailed results are presented in Tables 11 and 12.

<sup>2</sup>github: NetManAIOps/donut

<sup>3</sup>github: ahstat/affiliation-metrics-py

Table 7: Ablation Study of COGNOS Components and Filtering Methods on the PSM Dataset Across Various Backbones. The best results are highlighted in **bold**.

Dataset	PSM											
	COGNOS			$w/GWNR+MA$			$w/GWNR+LP$			$w/oGWNR+KS$		
	AP	AR	AF	AP	AR	AF	AP	AR	AF	AP	AR	AF
AnomalyT	0.941	<b>0.768</b>	<b>0.842</b>	0.947	0.685	0.782	0.934	0.663	0.769	0.946	0.554	0.679
Autoformer	0.915	<b>0.799</b>	<b>0.852</b>	0.906	0.753	0.818	0.965	0.698	0.800	0.897	0.640	0.727
Dlinear	0.887	<b>0.996</b>	<b>0.936</b>	0.871	0.959	0.910	0.905	0.946	0.924	0.888	0.990	0.934
FiLM	<b>0.920</b>	<b>0.996</b>	<b>0.956</b>	0.892	0.981	0.933	0.911	0.942	0.926	0.883	0.986	0.930
iTrans	0.884	<b>0.996</b>	<b>0.934</b>	0.867	0.963	0.910	<b>0.903</b>	0.939	0.920	0.889	0.948	0.917
LightTS	0.884	0.995	0.934	0.864	0.949	0.902	<b>0.910</b>	0.943	0.926	0.895	<b>0.996</b>	<b>0.941</b>
MICN	0.886	<b>0.998</b>	0.937	0.876	0.987	0.926	0.903	0.940	0.920	0.899	0.989	<b>0.941</b>
PatchTsT	0.894	<b>0.997</b>	<b>0.941</b>	0.892	0.976	0.931	0.915	0.933	0.924	0.885	0.978	0.927
Pyraformer	0.898	<b>0.825</b>	<b>0.860</b>	0.857	0.820	0.838	0.913	0.735	0.812	<b>0.941</b>	0.527	0.602
TimeMixer	0.901	<b>0.999</b>	<b>0.946</b>	0.893	0.972	0.930	0.911	0.953	0.931	0.881	0.978	0.925
TimesNet	0.895	<b>0.998</b>	0.942	0.906	0.992	<b>0.946</b>	0.923	0.846	0.883	0.910	0.968	0.937
Transformer	0.958	<b>0.767</b>	<b>0.846</b>	0.946	0.711	0.802	0.965	0.667	0.777	0.938	0.527	0.651
<b>AVG</b>	0.905	<b>0.928</b>	<b>0.910</b>	0.893	0.896	0.886	0.922	0.850	0.876	0.904	0.840	0.843

Table 8: Continued Table of Table 7

Dataset	PSM					
	$w/GWNR+w/oFilter$			$w/oGWNR+w/oFilter$		
	AP	AR	AF	AP	AR	AF
AnomalyT	0.961	0.580	0.696	<b>0.961</b>	0.561	0.675
Autoformer	0.998	0.524	0.635	<b>1.000</b>	0.464	0.576
Dlinear	<b>0.927</b>	0.580	0.691	0.923	0.665	0.763
FiLM	0.828	0.497	0.603	0.837	0.508	0.590
iTrans	0.866	0.567	0.672	0.866	0.616	0.711
LightTS	0.884	0.641	0.730	0.890	0.653	0.744
MICN	0.922	0.717	0.795	<b>0.957</b>	0.667	0.778
PatchTsT	0.913	0.589	0.696	<b>0.949</b>	0.624	0.737
Pyraformer	0.937	0.580	0.692	0.940	0.637	0.740
TimeMixer	0.875	0.525	0.619	<b>0.943</b>	0.635	0.743
TimesNet	0.866	0.593	0.691	<b>0.943</b>	0.757	0.833
Transformer	<b>0.977</b>	0.560	0.675	0.974	0.566	0.682
<b>AVG</b>	0.913	0.579	0.683	<b>0.932</b>	0.613	0.714

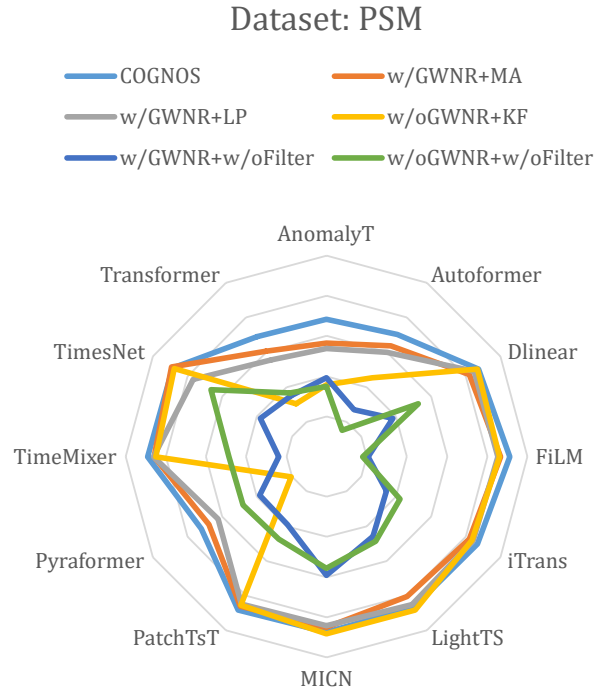


Figure 15: Average F-Score Performance

Table 9: Ablation Study of COGNOS Components and Filtering Methods on the MSL Dataset Across Various Backbones. The best results are highlighted in **bold**.

Dataset	MSL											
	COGNOS			$w/GWNR+MA$			$w/GWNR+LP$			$w/oGWNR+KS$		
	AP	AR	AF	AP	AR	AF	AP	AR	AF	AP	AR	AF
AnomalyT	<b>0.907</b>	<b>0.981</b>	<b>0.942</b>	0.893	0.946	0.917	0.864	0.872	0.865	0.858	0.907	0.879
Autoformer	<b>0.917</b>	<b>0.991</b>	<b>0.952</b>	0.878	0.941	0.906	0.863	0.873	0.865	0.872	0.936	0.901
Dlinear	0.902	0.981	0.939	0.865	0.884	0.871	0.870	0.884	0.874	<b>0.932</b>	<b>1.000</b>	<b>0.965</b>
FiLM	<b>0.878</b>	<b>0.951</b>	<b>0.912</b>	0.808	0.701	0.748	0.806	0.756	0.773	0.809	0.822	0.807
iTrans	0.905	0.981	0.941	0.862	0.887	0.871	0.878	0.908	0.890	<b>0.921</b>	<b>0.987</b>	<b>0.953</b>
LightTS	<b>0.929</b>	<b>1.000</b>	<b>0.963</b>	0.909	0.955	0.931	0.866	0.884	0.872	0.924	0.987	0.955
MICN	<b>0.908</b>	<b>0.981</b>	<b>0.942</b>	0.879	0.930	0.901	0.799	0.750	0.766	0.868	0.914	0.888
PatchTsT	0.922	0.999	0.959	0.862	0.880	0.868	0.864	0.880	0.869	<b>0.932</b>	<b>1.000</b>	<b>0.965</b>
Pyraformer	<b>0.923</b>	<b>1.000</b>	<b>0.960</b>	0.892	0.940	0.914	0.866	0.884	0.872	0.863	0.860	0.860
TimeMixer	<b>0.883</b>	<b>0.948</b>	<b>0.913</b>	0.826	0.812	0.817	0.790	0.617	0.677	0.870	0.921	0.893
TimesNet	<b>0.911</b>	<b>0.990</b>	<b>0.949</b>	0.875	0.919	0.894	0.864	0.884	0.871	0.911	0.972	0.940
Transformer	<b>0.917</b>	<b>0.989</b>	<b>0.952</b>	0.881	0.918	0.897	0.864	0.872	0.865	0.857	0.899	0.875
<b>AVG</b>	<b>0.908</b>	<b>0.982</b>	<b>0.944</b>	0.869	0.893	0.878	0.850	0.838	0.838	0.885	0.934	0.907

Table 10: Continued Table of Table 9

Dataset	MSL					
	$w/GWNR+w/oFilter$			$w/oGWNR+w/oFilter$		
	AP	AR	AF	AP	AR	AF
AnomalyT	0.863	0.375	0.517	0.873	0.378	0.522
Autoformer	0.869	0.440	0.571	0.870	0.441	0.572
Dlinear	0.809	0.220	0.345	0.831	0.456	0.580
FiLM	0.800	0.158	0.262	0.814	0.194	0.314
iTrans	0.718	0.113	0.195	0.844	0.426	0.551
LightTS	0.853	0.367	0.507	0.843	0.450	0.577
MICN	0.852	0.373	0.512	0.852	0.371	0.511
PatchTsT	0.728	0.118	0.204	0.844	0.456	0.575
Pyraformer	0.868	0.411	0.548	0.868	0.411	0.548
TimeMixer	0.793	0.180	0.289	0.828	0.458	0.581
TimesNet	0.851	0.376	0.516	0.855	0.444	0.571
Transformer	0.863	0.375	0.517	0.874	0.379	0.522
<b>AVG</b>	0.822	0.292	0.415	0.850	0.405	0.535

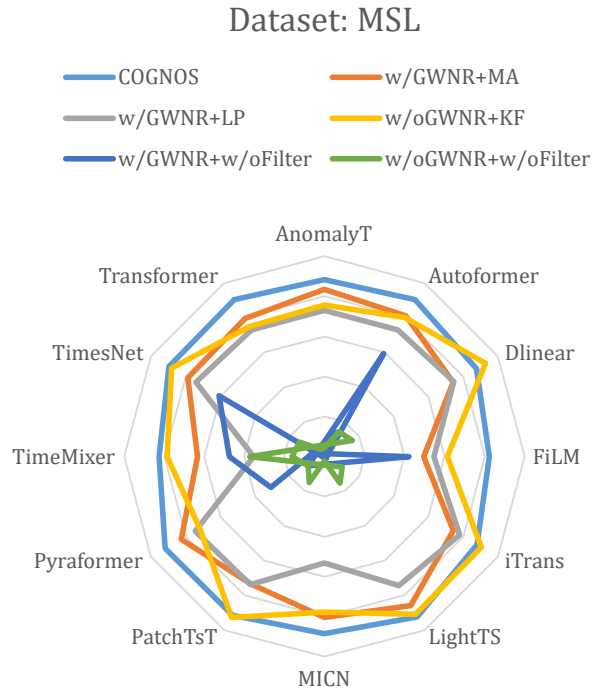


Figure 16: Average F-Score Performance

Table 11: Full results of the proposed COGNOS compare to Vanilla MSE method on SWaT and MSL datasets. we use Adjusted metrics and Affiliation metrics to calculate precision (P), recall (R) and F-score (F). The best results are highlighted in **bold**.

Datasets		SWaT						MSL					
Models	METRIC	Vanilla			COGNOS			Vanilla			COGNOS		
		P	R	F	P	R	F	P	R	F	P	R	F
AnomalyT	Adjusted	<b>0.998</b>	0.661	0.795	0.902	<b>0.891</b>	<b>0.896</b>	<b>0.935</b>	0.493	0.646	0.934	<b>0.969</b>	<b>0.951</b>
	Affiliation	0.818	0.029	0.055	<b>0.858</b>	<b>0.698</b>	<b>0.769</b>	0.811	0.263	0.397	<b>0.880</b>	<b>0.992</b>	<b>0.933</b>
	<b>AVG</b>	<b>0.908</b>	0.345	0.425	0.880	<b>0.794</b>	<b>0.833</b>	0.873	0.378	0.522	<b>0.907</b>	<b>0.981</b>	<b>0.942</b>
Autoformer	Adjusted	<b>1.000</b>	0.656	0.792	0.937	<b>0.815</b>	<b>0.872</b>	<b>0.947</b>	0.619	0.749	0.929	<b>0.984</b>	<b>0.956</b>
	Affiliation	0.888	0.003	0.006	<b>0.894</b>	<b>0.513</b>	<b>0.652</b>	0.792	0.263	0.394	<b>0.904</b>	<b>0.997</b>	<b>0.948</b>
	<b>AVG</b>	<b>0.944</b>	0.329	0.399	0.916	<b>0.664</b>	<b>0.762</b>	0.870	0.441	0.572	<b>0.917</b>	<b>0.991</b>	<b>0.952</b>
Dlinear	Adjusted	0.923	<b>0.931</b>	<b>0.927</b>	<b>0.937</b>	0.817	0.873	<b>0.931</b>	0.622	0.746	0.926	<b>0.969</b>	<b>0.947</b>
	Affiliation	0.698	0.396	0.505	<b>0.897</b>	<b>0.514</b>	<b>0.654</b>	0.730	0.290	0.415	<b>0.877</b>	<b>0.992</b>	<b>0.931</b>
	<b>AVG</b>	0.810	0.663	0.716	<b>0.917</b>	<b>0.666</b>	<b>0.763</b>	0.831	0.456	0.580	<b>0.902</b>	<b>0.981</b>	<b>0.939</b>
FiLM	Adjusted	<b>0.919</b>	0.864	0.890	0.893	<b>0.991</b>	<b>0.939</b>	0.819	0.202	0.324	<b>0.925</b>	<b>0.923</b>	<b>0.924</b>
	Affiliation	0.661	0.218	0.328	<b>0.866</b>	<b>0.987</b>	<b>0.923</b>	0.808	0.186	0.303	<b>0.832</b>	<b>0.978</b>	<b>0.899</b>
	<b>AVG</b>	0.790	0.541	0.609	<b>0.879</b>	<b>0.989</b>	<b>0.931</b>	0.814	0.194	0.314	<b>0.878</b>	<b>0.951</b>	<b>0.912</b>
iTrans	Adjusted	<b>0.922</b>	0.931	0.926	0.865	<b>1.000</b>	<b>0.928</b>	0.925	0.611	0.736	<b>0.929</b>	<b>0.969</b>	<b>0.948</b>
	Affiliation	0.745	0.398	0.519	<b>0.864</b>	<b>1.000</b>	<b>0.927</b>	0.763	0.240	0.365	<b>0.881</b>	<b>0.992</b>	<b>0.933</b>
	<b>AVG</b>	0.834	0.664	0.722	<b>0.865</b>	<b>1.000</b>	<b>0.928</b>	0.844	0.426	0.551	<b>0.905</b>	<b>0.981</b>	<b>0.941</b>
LightTS	Adjusted	<b>0.923</b>	<b>0.932</b>	<b>0.928</b>	0.874	0.864	0.869	<b>0.934</b>	0.622	0.747	0.933	<b>1.000</b>	<b>0.966</b>
	Affiliation	0.749	0.407	0.527	<b>0.793</b>	<b>0.729</b>	<b>0.759</b>	0.753	0.278	0.407	<b>0.924</b>	<b>1.000</b>	<b>0.960</b>
	<b>AVG</b>	<b>0.836</b>	0.669	0.727	0.833	<b>0.797</b>	<b>0.814</b>	0.843	0.450	0.577	<b>0.929</b>	<b>1.000</b>	<b>0.963</b>
MICN	Adjusted	<b>0.919</b>	0.951	0.935	0.901	<b>1.000</b>	<b>0.948</b>	0.913	0.489	0.637	<b>0.931</b>	<b>0.969</b>	<b>0.950</b>
	Affiliation	0.716	0.576	0.638	<b>0.890</b>	<b>1.000</b>	<b>0.942</b>	0.791	0.254	0.384	<b>0.885</b>	<b>0.993</b>	<b>0.935</b>
	<b>AVG</b>	0.818	0.764	0.787	<b>0.896</b>	<b>1.000</b>	<b>0.945</b>	0.852	0.371	0.511	<b>0.908</b>	<b>0.981</b>	<b>0.942</b>
PatchTsT	Adjusted	<b>0.910</b>	0.798	0.850	0.868	<b>1.000</b>	<b>0.929</b>	<b>0.936</b>	0.663	0.776	0.932	<b>0.997</b>	<b>0.964</b>
	Affiliation	0.736	0.217	0.335	<b>0.866</b>	<b>1.000</b>	<b>0.928</b>	0.751	0.249	0.374	<b>0.912</b>	<b>1.000</b>	<b>0.954</b>
	<b>AVG</b>	0.823	0.507	0.593	<b>0.867</b>	<b>1.000</b>	<b>0.929</b>	0.844	0.456	0.575	<b>0.922</b>	<b>0.999</b>	<b>0.959</b>
Pyraformer	Adjusted	<b>0.998</b>	0.656	0.792	0.919	<b>0.844</b>	<b>0.880</b>	<b>0.942</b>	0.562	0.704	0.929	<b>1.000</b>	<b>0.963</b>
	Affiliation	0.628	0.015	0.030	<b>0.880</b>	<b>0.543</b>	<b>0.671</b>	0.795	0.259	0.391	<b>0.916</b>	<b>1.000</b>	<b>0.956</b>
	<b>AVG</b>	0.813	0.336	0.411	<b>0.899</b>	<b>0.693</b>	<b>0.776</b>	0.868	0.411	0.548	<b>0.923</b>	<b>1.000</b>	<b>0.960</b>
TimeMixer	Adjusted	<b>0.976</b>	0.797	0.877	0.965	<b>1.000</b>	<b>0.982</b>	<b>0.933</b>	0.630	0.752	0.928	<b>0.929</b>	<b>0.928</b>
	Affiliation	0.781	0.201	0.320	<b>0.955</b>	<b>1.000</b>	<b>0.977</b>	0.722	0.286	0.410	<b>0.837</b>	<b>0.967</b>	<b>0.898</b>
	<b>AVG</b>	0.878	0.499	0.599	<b>0.960</b>	<b>1.000</b>	<b>0.980</b>	0.828	0.458	0.581	<b>0.883</b>	<b>0.948</b>	<b>0.913</b>
TimesNet	Adjusted	<b>0.921</b>	0.931	0.926	0.863	<b>1.000</b>	<b>0.927</b>	<b>0.932</b>	0.621	0.746	0.928	<b>0.984</b>	<b>0.955</b>
	Affiliation	0.734	0.430	0.543	<b>0.864</b>	<b>1.000</b>	<b>0.927</b>	0.779	0.267	0.397	<b>0.894</b>	<b>0.996</b>	<b>0.942</b>
	<b>AVG</b>	0.828	0.681	0.734	<b>0.864</b>	<b>1.000</b>	<b>0.927</b>	0.855	0.444	0.571	<b>0.911</b>	<b>0.990</b>	<b>0.949</b>
Transformer	Adjusted	<b>0.998</b>	0.661	0.795	0.905	<b>0.904</b>	<b>0.905</b>	<b>0.935</b>	0.494	0.646	0.934	<b>0.984</b>	<b>0.959</b>
	Affiliation	0.839	0.030	0.057	<b>0.882</b>	<b>0.713</b>	<b>0.789</b>	0.812	0.264	0.398	<b>0.900</b>	<b>0.995</b>	<b>0.945</b>
	<b>AVG</b>	<b>0.918</b>	0.345	0.426	0.894	<b>0.809</b>	<b>0.847</b>	0.874	0.379	0.522	<b>0.917</b>	<b>0.989</b>	<b>0.952</b>
<b>AVG</b>		0.850	0.529	0.596	<b>0.889</b>	<b>0.868</b>	<b>0.869</b>	0.850	0.405	0.535	<b>0.908</b>	<b>0.982</b>	<b>0.944</b>

Table 12: Full results of the proposed COGNOS compare to Vanilla MSE method on PSM and SMAP datasets. we use Adjusted metrics and Affiliation metrics to calculate precision (P), recall (R) and F-score (F). The best results are highlighted in **bold**.

Datasets		PSM						SMAP					
Models	METRIC	Vanilla			COGNOS			Vanilla			COGNOS		
		P	R	F	P	R	F	P	R	F	P	R	F
AnomalyT	Adjusted	<b>0.995</b>	0.828	0.904	0.979	<b>0.902</b>	<b>0.939</b>	<b>0.943</b>	0.540	0.687	0.928	<b>0.595</b>	<b>0.725</b>
	Affiliation	<b>0.927</b>	0.294	0.447	0.904	<b>0.633</b>	<b>0.745</b>	<b>0.728</b>	0.194	0.307	0.706	<b>0.843</b>	<b>0.768</b>
	AVG	<b>0.961</b>	0.561	0.675	0.941	<b>0.768</b>	<b>0.842</b>	<b>0.835</b>	0.367	0.497	0.817	<b>0.719</b>	<b>0.747</b>
Autoformer	Adjusted	<b>1.000</b>	0.759	0.863	0.975	<b>0.910</b>	<b>0.941</b>	0.953	0.618	0.750	<b>0.956</b>	<b>0.919</b>	<b>0.938</b>
	Affiliation	<b>0.999</b>	0.169	0.289	0.855	<b>0.688</b>	<b>0.763</b>	0.827	0.215	0.341	<b>0.870</b>	<b>0.987</b>	<b>0.925</b>
	AVG	<b>1.000</b>	0.464	0.576	0.915	<b>0.799</b>	<b>0.852</b>	0.890	0.416	0.545	<b>0.913</b>	<b>0.953</b>	<b>0.931</b>
Dlinear	Adjusted	<b>0.992</b>	0.865	0.924	0.979	<b>0.999</b>	<b>0.989</b>	<b>0.949</b>	0.526	0.677	0.931	<b>0.603</b>	<b>0.732</b>
	Affiliation	<b>0.853</b>	0.465	0.602	0.795	<b>0.994</b>	<b>0.883</b>	<b>0.840</b>	0.182	0.299	0.769	<b>0.862</b>	<b>0.813</b>
	AVG	<b>0.923</b>	0.665	0.763	0.887	<b>0.996</b>	<b>0.936</b>	<b>0.894</b>	0.354	0.488	0.850	<b>0.733</b>	<b>0.773</b>
FiLM	Adjusted	0.988	0.851	0.915	<b>0.988</b>	<b>0.999</b>	<b>0.994</b>	<b>0.946</b>	0.506	0.660	0.938	<b>0.657</b>	<b>0.773</b>
	Affiliation	0.686	0.164	0.265	<b>0.852</b>	<b>0.993</b>	<b>0.917</b>	<b>0.804</b>	0.102	0.180	0.660	<b>0.758</b>	<b>0.706</b>
	AVG	0.837	0.508	0.590	<b>0.920</b>	<b>0.996</b>	<b>0.956</b>	<b>0.875</b>	0.304	0.420	0.799	<b>0.708</b>	<b>0.739</b>
iTrans	Adjusted	<b>0.987</b>	0.841	0.908	0.977	<b>0.999</b>	<b>0.988</b>	<b>0.954</b>	0.508	0.663	0.942	<b>0.714</b>	<b>0.812</b>
	Affiliation	0.745	0.392	0.513	<b>0.791</b>	<b>0.992</b>	<b>0.880</b>	0.690	0.124	0.210	<b>0.779</b>	<b>0.843</b>	<b>0.810</b>
	AVG	0.866	0.616	0.711	<b>0.884</b>	<b>0.996</b>	<b>0.934</b>	0.822	0.316	0.437	<b>0.860</b>	<b>0.778</b>	<b>0.811</b>
LightTS	Adjusted	<b>0.990</b>	0.871	0.927	0.978	<b>0.999</b>	<b>0.989</b>	<b>0.949</b>	0.528	0.679	0.929	<b>0.597</b>	<b>0.727</b>
	Affiliation	0.791	0.435	0.561	<b>0.791</b>	<b>0.991</b>	<b>0.880</b>	<b>0.809</b>	0.179	0.292	0.752	<b>0.845</b>	<b>0.796</b>
	AVG	<b>0.890</b>	0.653	0.744	0.884	<b>0.995</b>	<b>0.934</b>	<b>0.879</b>	0.353	0.486	0.841	<b>0.721</b>	<b>0.761</b>
MICN	Adjusted	<b>0.994</b>	0.827	0.903	0.977	<b>0.999</b>	<b>0.988</b>	<b>0.946</b>	0.517	0.668	0.932	<b>0.597</b>	<b>0.728</b>
	Affiliation	<b>0.920</b>	0.506	0.653	0.796	<b>0.998</b>	<b>0.885</b>	<b>0.750</b>	0.158	0.261	0.680	<b>0.754</b>	<b>0.715</b>
	AVG	<b>0.957</b>	0.667	0.778	0.886	<b>0.998</b>	<b>0.937</b>	<b>0.848</b>	0.337	0.465	0.806	<b>0.676</b>	<b>0.721</b>
PatchTsT	Adjusted	<b>0.996</b>	0.835	0.909	0.978	<b>1.000</b>	<b>0.989</b>	<b>0.950</b>	0.549	0.696	0.945	<b>0.749</b>	<b>0.836</b>
	Affiliation	<b>0.903</b>	0.412	0.566	0.809	<b>0.995</b>	<b>0.893</b>	0.788	0.205	0.325	<b>0.827</b>	<b>0.914</b>	<b>0.869</b>
	AVG	<b>0.949</b>	0.624	0.737	0.894	<b>0.997</b>	<b>0.941</b>	0.869	0.377	0.511	<b>0.886</b>	<b>0.832</b>	<b>0.852</b>
Pyraformer	Adjusted	<b>0.998</b>	0.883	0.937	0.971	<b>0.914</b>	<b>0.942</b>	0.945	0.541	0.688	<b>0.958</b>	<b>0.923</b>	<b>0.940</b>
	Affiliation	<b>0.881</b>	0.392	0.543	0.825	<b>0.737</b>	<b>0.779</b>	0.762	0.182	0.294	<b>0.864</b>	<b>0.952</b>	<b>0.906</b>
	AVG	<b>0.940</b>	0.637	0.740	0.898	<b>0.825</b>	<b>0.860</b>	0.853	0.362	0.491	<b>0.911</b>	<b>0.937</b>	<b>0.923</b>
TimeMixer	Adjusted	<b>0.995</b>	0.855	0.920	0.978	<b>0.999</b>	<b>0.989</b>	<b>0.954</b>	0.554	0.701	0.950	<b>0.849</b>	<b>0.897</b>
	Affiliation	<b>0.891</b>	0.414	0.565	0.824	<b>0.998</b>	<b>0.903</b>	0.833	0.235	0.367	<b>0.857</b>	<b>0.935</b>	<b>0.895</b>
	AVG	<b>0.943</b>	0.635	0.743	0.901	<b>0.999</b>	<b>0.946</b>	0.893	0.395	0.534	<b>0.904</b>	<b>0.892</b>	<b>0.896</b>
TimesNet	Adjusted	<b>0.993</b>	0.935	0.963	0.976	<b>0.999</b>	<b>0.987</b>	0.945	0.525	0.675	<b>0.949</b>	<b>0.801</b>	<b>0.869</b>
	Affiliation	<b>0.894</b>	0.578	0.702	0.814	<b>0.998</b>	<b>0.897</b>	0.805	0.173	0.285	<b>0.863</b>	<b>0.947</b>	<b>0.903</b>
	AVG	<b>0.943</b>	0.757	0.833	0.895	<b>0.998</b>	<b>0.942</b>	0.875	0.349	0.480	<b>0.906</b>	<b>0.874</b>	<b>0.886</b>
Transformer	Adjusted	<b>0.999</b>	0.831	0.907	0.979	<b>0.919</b>	<b>0.948</b>	0.945	0.544	0.690	<b>0.945</b>	<b>0.749</b>	<b>0.836</b>
	Affiliation	<b>0.950</b>	0.301	0.457	0.938	<b>0.615</b>	<b>0.743</b>	0.763	0.218	0.339	<b>0.829</b>	<b>0.918</b>	<b>0.872</b>
	AVG	<b>0.974</b>	0.566	0.682	0.958	<b>0.767</b>	<b>0.846</b>	0.854	0.381	0.515	<b>0.887</b>	<b>0.834</b>	<b>0.854</b>
AVG		<b>0.932</b>	0.613	0.714	0.905	<b>0.928</b>	<b>0.910</b>	<b>0.866</b>	0.359	0.489	0.865	<b>0.805</b>	<b>0.824</b>